

 Open access • Posted Content • DOI:10.1101/2021.07.05.451168

Feeding effects on liver mitochondrial bioenergetics of *Boa constrictor* (Serpentes: Boidae) — [Source link](#)

[Helena Rachel da Mota Araujo](#), [Marina R. Sartori](#), [Claudia D. C. Navarro](#), [J. E. de Carvalho](#) ...+1 more authors

Institutions: [Federal University of Bahia](#), [State University of Campinas](#), [Federal University of São Paulo](#)

Published on: 05 Jul 2021 - [bioRxiv](#) (Cold Spring Harbor Laboratory)

Topics: [Boa constrictor](#), [Bioenergetics](#), [Mitochondrial permeability transition pore](#) and [Citrate synthase](#)

Related papers:

- [Feeding effects on liver mitochondrial bioenergetics of *Boa constrictor* \(Serpentes: Boidae\).](#)
- [Patterns of energetic substrate modifications in response to feeding in boas, *Boa constrictor* \(Serpentes, Boidae\).](#)
- [Physiological adaptations to reproduction. II. Mitochondrial adjustments in livers of lactating mice.](#)
- [Mitochondrial oxidative phosphorylation efficiency is upregulated during fasting in two major oxidative tissues of ducklings](#)
- [The effect of aging and caloric restriction on mitochondrial protein density and oxygen consumption](#)

Share this paper:    

View more about this paper here: <https://typeset.io/papers/feeding-effects-on-liver-mitochondrial-bioenergetics-of-boa-3h1h5gudyc>

26 ABSTRACT

27 Snakes are interesting examples of overcoming energy metabolism challenges as many
28 species can endure long periods without feeding, and their eventual meals are of
29 reasonably large sizes, thus exhibiting dual extreme adaptations. Consequently,
30 metabolic rate increases considerably to attend to the energetic demand of digestion,
31 absorption and, protein synthesis. These animals should be adapted to transition from
32 these two opposite states of energy fairly quickly, and therefore we investigated
33 mitochondrial function plasticity in these states. Herein we compared liver
34 mitochondrial bioenergetics of the boid snake *Boa constrictor* during fasting and after
35 meal intake. We fasted the snakes for 60 days, then we fed a subgroup with 30% of their
36 body size and evaluated their maximum postprandial response. We measured liver
37 respiration rates from permeabilized tissue and isolated mitochondria, and from isolated
38 mitochondria, we also measured Ca^{2+} retention capacity, the release of H_2O_2 , and
39 NAD(P) redox state. Mitochondrial respiration rates were maximized after feeding,
40 reaching until 60% increase from fasting levels when energized with complex I-linked
41 substrates. Interestingly, fasting and fed snakes exhibited similar respiratory control
42 ratios and citrate synthase activity. Furthermore, we found no differences in Ca^{2+}
43 retention capacity, indicating no increase in susceptibility to mitochondrial permeability
44 transition pore (PTP), or redox state of NAD(P), although fed animals exhibited
45 increases in the release of H_2O_2 . Thus, we conclude that liver mitochondria from *B.*
46 *constrictor* snakes increase the maintenance costs during the postprandial period and
47 quickly improve the mitochondrial bioenergetics capacity without compromising the
48 redox balance.

49 **Keywords:** fasting, specific dynamic action, liver mitochondria, calcium retention
50 capacity, permeability transition pore, redox balance

51

52 INTRODUCTION

53

54 Mitochondria are complex and dynamic organelles present in eukaryotic cells
55 responsible for energy production and cellular homeostasis. They play a fundamental
56 role in the balance of energetic homeostasis upon intracellular signaling, apoptosis,
57 metabolism of amino acids, lipids, cholesterol, steroids, and nucleotides, and its primary
58 known function of oxidation of energetic substrates and ATP production (Duchen,

59 2000). This energy expenditure at the cellular level needs to be finely tuned to the
60 varying availability of energy substrates from food resources and energetic demand
61 from activities to allow better organismal performance. Animals can face challenges due
62 to environmental changes as seasonal scarcity of food, behavior or life-history traits,
63 increasing energy expenditure, like reproduction and migration. One basic regulation of
64 energy expenditure depends on the control of oxidative phosphorylation, as this process
65 accounts for most of the whole-animal oxygen consumption and has a considerable
66 effect on cellular respiration flux (Benard et al., 2006; Brown et al., 1990; Dejean et al.,
67 2001; Rolfe and Brown, 1997).

68 Ambush-foraging snakes are commonly used as experimental model organisms
69 because of their resistance to long periods of food deprivation and the magnitude of
70 their physiological responses after feeding large meals (Secor and Diamond, 1998;
71 Starck and Beese, 2001; McCue et al., 2012). These snakes survive exceptional long
72 periods of fasting by employing different strategies for energy conservation, as
73 reduction in metabolic rates, organ mass and activity, and control of the mobilization of
74 fuel sources (McCue, 2007; McCue et al., 2012). On the other hand, once fed, ambush-
75 foraging snakes exhibit a remarkable increase in the metabolism, of comparatively
76 higher magnitude than other animals (Secor and Diamond, 1998). The postprandial
77 metabolic increment after meal intake (termed Specific Dynamic Action or SDA;
78 Kleiber, 1961) may last for several days, depending on temperature regime, meal size,
79 and quality (Andrade et al., 2004; Cruz-Neto et al., 1999; Gavira and Andrade, 2013;
80 Secor and Diamond, 1997). Such elevated metabolism after feeding is mostly, if not
81 fully fueled by aerobic metabolism. Thus, studies of the modulation of energy pathways
82 involving oxidation of substrates ultimately leading to consumption of oxygen and
83 production of ATP through the mitochondrial respiratory chain are essential to
84 understand the regulation of metabolism at a cellular level.

85 In endothermic vertebrates, research has mainly focused on the mitochondrial
86 effects of fasting, and studies conducted in mammals and birds report that food
87 deprivation is accompanied by decreased mitochondrial respiration rates and increased
88 rates of reactive oxygen species (ROS) production (Bourguignon et al., 2017; Dumas et
89 al., 2004; Menezes-Filho et al., 2019; Roussel et al., 2019; Sorensen et al., 2006).
90 Mitochondria unwittingly generate ROS as a by-product, and at low levels serves as
91 redox signaling molecules, allowing adaptation to changes in environmental nutrients
92 and oxidative environment (Schieber and Chandel, 2014; Shadel and Horvath, 2015).

93 However, an excess can exhaust the antioxidant system and promote damage to
94 proteins, lipids, and DNA, leading to oxidative stress (Hamanaka and Chandel, 2010).
95 However, in species adapted to prolonged fasting, including mammalian hibernators,
96 there seem to be mechanisms that allow the mitigation of oxidative stress (Ensminger et
97 al., 2021). Nevertheless, although a robust body of literature exists for the physiological
98 effects of fasting and feeding in snakes (McCue, 2008; Secor, 2009), knowledge of the
99 optimization of metabolism at the subcellular level during periods of fasting or during
100 the metabolic increment after meal intake are lacking (Butler et al., 2016).

101 We hypothesize that snakes will display mitochondrial plasticity, exhibiting an
102 increase in the capacity for ATP generation during the postprandial period following the
103 increase in energetic demand of digestion and absorption. To test this, we investigated
104 the liver mitochondrial function and redox balance after 60-days of fasting and during
105 the postprandial period in the ambush-foraging boid snake *Boa constrictor*. This
106 neotropical snake feed infrequently, surviving periods of fasting longer than two months
107 (McCue and Pollock, 2008), that can ingest large meals, exhibiting large increments in
108 aerobic metabolic rate (Andrade et al., 2004; de Figueiredo et al., 2020; Toledo et al.,
109 2003). As the liver plays a vital role in snake's metabolism, participating in the
110 oxidation of triglycerides, synthesis of cholesterol, lipoprotein and aminoacids, and
111 control of blood sugar levels, it is relevant to assess the contribution of this organ to
112 overall energetic demand after meal intake. In boas, the liver exhibit increased mass
113 (Secor and Diamond, 2000) and a larger volume of glycogen granules two days post-
114 feeding (da Mota Araujo, unpublished data). Thus, we compared mitochondrial liver
115 bioenergetics of fasted and fed *B. constrictor*, evaluating mitochondrial respiration,
116 calcium retention capacity, ROS release, and NAD(P) redox state.

117

118 MATERIAL AND METHODS

119

120 Reagents

121 We purchased the fluorescent probes Calcium GreenTM-5N and AmplexTM UltraRed
122 from Thermo Fischer Scientific (Eugene, OR, USA) and dissolved in deionized water
123 and dimethyl sulfoxide (DMSO), respectively. All other chemicals were obtained from
124 Sigma-Aldrich (Saint Louis, MO, USA). Stock solutions of respiratory substrates and
125 nucleotides were prepared in a 20 mM HEPES solution with the pH adjusted to 7.2
126 using KOH.

127

128 **Animals**

129 We obtained juvenile snakes *Boa constrictor* Linnaeus, 1758 (N = 9, body mass =
130 152.09 ± 15.96 ; total length = 73.72 ± 3.35 cm, mean \pm s.d.) from Centro de
131 Recuperação de Animais Silvestres do Parque Ecológico do Tietê (CRAS, São Paulo,
132 SP, Brazil). We housed the animals in individual boxes (56.4 l \times 38.5 w \times 20.1 h cm)
133 with venting holes in the lid, under natural light and temperature ($25 \pm 2^\circ\text{C}$, mean \pm s.d.)
134 with free access to water. Initially, we fed all animals with mice (*Mus musculus*) to
135 standardize the beginning of the treatment (with the equivalent of 5% of their body
136 masses). After, we kept all snakes in fasting for two months. Then, we divided the
137 snakes into two groups: fasting (N = 5) and fed (N = 4). We fed the snakes of the ‘fed
138 group’ with mice accounting for 30% of their body weight and euthanized them 2 days
139 after prey ingestion, usually when the maximum VO_2 (oxygen consumption) is achieved
140 (peak SDA; Secor and Diamond, 2000; de Figueiredo et al., 2020). We performed all
141 measurements at the Laboratory of Bioenergetics at Universidade Estadual de Campinas
142 (UNICAMP), Campinas, SP, Brazil. We anesthetized the snakes with isoflurane and
143 sectioned the medulla after cessation of reflexes. All experimental procedures were
144 approved by the Local Committee for Ethics in Animal Experimentation
145 (CEUA/UNICAMP: 5301-1/2019) and complied with the ARRIVE guidelines. The use
146 of *Boa constrictor* was authorized by the Brazilian Institute for Environment (SISBIO;
147 number 69655-1).

148

149 **Permeabilized liver tissue**

150 We rapidly removed a portion of the liver and immersed in ice-cold BIOPS buffer (10
151 mM Ca-EGTA buffer [2.77 mM of CaK_2EGTA C 7.23 mM of K_2EGTA , free
152 concentration of calcium 0.1 mM], 20 mM imidazole, 50 mM KC/ 4-
153 morpholinoethanesulfonic acid, 0.5 mM dithiothreitol, 7 mM MgCl_2 , 5 mM ATP, 15
154 mM phosphocreatine, pH 7.1). Then we permeabilized liver samples of 8 to 10 mg
155 tissue in ice-cold buffer containing saponin ($0.5 \text{ mg} \cdot \text{mL}^{-1}$) during 30 min, gently stirred
156 and washed with MIR05 medium (60 mM potassium lactobionate, 1 mM MgCl_2 , 20
157 mM taurine, 10 mM KH_2PO_4 , 20 mM HEPES, 110 mM sucrose, $1 \text{ g} \cdot \text{L}^{-1}$ BSA, pH 7.1)
158 at 4°C . We dried the samples with filter paper and weighted (Busanello et al., 2017;
159 Kuznetsov et al., 2008) before respirometric measurements.

160

161 **Mitochondrial isolation**

162 We isolated liver mitochondria by conventional differential centrifugation (Ronchi et
163 al., 2013). Briefly, we rapidly removed the liver, finely minced and homogenized in ice-
164 cold isolation medium containing 250 mM sucrose, 1 mM EGTA, and 10 mM HEPES
165 buffer (pH 7.2). We centrifuged the homogenate for 10 min at 800 g. Then, we
166 centrifuged the collected supernatant at 7,750 g for 10 min. We resuspended the
167 resulting pellet in buffer containing 250 mM sucrose, 0.3 mM EGTA, and 10 mM
168 HEPES buffer (pH 7.2), and centrifuged again at 7,750 g for 10 min. We resuspended
169 the final pellet containing liver mitochondria in an EGTA-free buffer at an approximate
170 protein concentration of $60 \text{ mg} \cdot \text{mL}^{-1}$, quantified by the Bradford method using bovine
171 serum albumin (BSA) as standards.

172

173 **Mitochondrial oxygen consumption**

174 We measured mitochondrial respiration by monitoring the rates of oxygen consumption
175 using a high-resolution oxygraph OROBOROS (Innsbruck, Austria), equipped with a
176 magnetic stirrer, in a temperature-controlled chamber maintained at 30°C for
177 permeabilized tissue and 28°C for isolated mitochondria. We suspended the
178 permeabilized liver tissues in 2 mL of MIR-05 supplemented with 300 μM EGTA and 5
179 mM malate, 10 mM pyruvate, and 10 mM glutamate. After measuring the basal O_2
180 consumption, respiration linked to oxidative phosphorylation (OXPHOS) was elicited
181 by the addition of 400 μM of ADP. Then, we added 1 $\mu\text{g} \cdot \text{mL}^{-1}$ of oligomycin to cease
182 the phosphorylation by ATP synthase (state 4_o), slowing down oxygen consumption.
183 Finally, we titrated carbonyl cyanide 4-(trifluoromethoxy) phenylhydrazone (FCCP)
184 until maximal electron transport system capacity that occurred at the concentration of
185 800 ηM , eliciting maximal respiration rate (ETS, V_{max}).

186 We suspended the isolated liver mitochondria ($0.5 \text{ mg} \cdot \text{mL}^{-1}$) in 2 mL of
187 standard reaction medium (125 mM sucrose, 65 mM KCl, 2 mM KH_2PO_4 , 1 mM
188 MgCl_2 , 10 mM HEPES buffer with the pH adjusted to 7.2 with KOH) supplemented
189 with 200 μM EGTA and 1 mM malate, 2.5 mM pyruvate and 2.5 mM glutamate to
190 evaluate respiration at complex I, with additions of 300 μM of ADP, 1 $\mu\text{g}/\text{mL}$ of
191 oligomycin and titration of FCCP, that elicited maximal respiration rate at 100 ηM . For
192 isolated mitochondria we applied an additional protocol for the evaluation of the
193 different mitochondrial complexes. We measured basal respiration with complex I-
194 linked substrates (5 mM malate, 10 mM pyruvate and 10 mM glutamate), followed by

195 the addition of ADP and FCCP as described above, then we added 1 μM rotenone to
196 block complex-I followed by the addition of 5 mM succinate to stimulate complex II.
197 Because the addition of 1 μM antimycin A or 1 μM myxothiazol were without effect on
198 blocking complex III, we discarded the final addition of 1 mM *N,N,N',N'*-tetramethyl-*p*-
199 phenylenediamine (TMPD) plus 100 μM ascorbate aimed for stimulation of complex
200 IV.

201

202 **Assessment of mitochondrial Ca^{2+} retention capacity**

203 We suspended liver mitochondria ($0.5 \text{ mg} \cdot \text{mL}^{-1}$) in standard reaction medium
204 supplemented with 10 μM EGTA, 0.2 μM of a calcium indicator (Calcium GreenTM-5N)
205 and respiratory substrates (1 mM malate, 2.5 mM pyruvate, and 2.5 mM glutamate). We
206 continuously monitored the fluorescence in a spectrofluorometer (Hitachi F-4500,
207 Tokyo, Japan) at 28°C using excitation and emission wavelengths of 506 and 532 nm,
208 respectively, and slit widths of 5 nm. We performed repeated pulses of CaCl_2 additions
209 (60 μM) after mitochondria were added to the system. We measured the amount of
210 CaCl_2 added before the start of Ca^{2+} release by mitochondria into the medium as an
211 index of the susceptibility to Ca^{2+} -induced PTP, confirmed by the assessment of the
212 PTP in the presence of 1 μM cyclosporine A (CsA). We converted the raw fluorescence
213 readings into Ca^{2+} concentration levels (expressed as micromolar) according to the
214 hyperbolic equation: $[\text{Ca}^{2+}] = K_d \times [(F - F_{\min}) / (F_{\max} - F)]$, where F is any given
215 fluorescence, F_{\min} is the lowest fluorescence reading after addition of 0.5 mM EGTA,
216 and F_{\max} is the maximal fluorescence obtained after two sequential additions of 1 mM
217 CaCl_2 . We performed these additions of EGTA and Ca^{2+} at the end of each trace. We
218 experimentally determined the dissociation constant (K_d) of 26.8 μM for the probe
219 Calcium GreenTM-5N in the incubation condition, as previously described (Sartori et al.,
220 2021).

221

222 **Citrate synthase activity**

223 We measured the catalytic activity of the enzyme citrate synthase in mitochondrial
224 samples monitoring the conversion of oxaloacetate and acetyl-CoA to citrate and CoA–
225 SH and by measuring the formation of the colorimetric product thionitrobenzoic acid
226 (TNB) at 412 nm and 37°C (Shepherd and Garland, 1969) on a microplate reader
227 (Power Wave XS-2, Biotek Instruments, Winooski, USA). We calculated the enzyme
228 activity using the changes in absorbance after substrate (250 μM oxaloacetate) addition

229 to the assay buffer (10 mM Trizma pH 8.0) containing 50 μ M acetyl-CoA and 100 μ M
230 DTNB.

231

232 **Hydrogen Peroxide (H₂O₂) release**

233 We monitored the H₂O₂ released by isolated liver mitochondria by the conversion of
234 Amplex™ UltraRed to fluorescent resorufin in the presence of horseradish peroxidase
235 (HRP). We incubated the suspensions of mitochondria from fasting and fed snakes (0.5
236 mg · mL⁻¹) in a reaction medium containing complex-I substrates (1 mM malate, 2.5
237 mM pyruvate, and 2.5 mM glutamate), 10 μ M Amplex™ UltraRed, 1 U · mL⁻¹ HRP and
238 30 U · mL⁻¹ superoxide dismutase (SOD). Additionally, we added 100 μ M phenylmethyl
239 sulfonyl fluoride (PMSF) to inhibit the conversion of amplex red by carboxylesterase
240 independent of H₂O₂ (Miwa et al., 2016). We monitored the fluorescence over time with
241 a temperature-controlled spectrofluorometer at 28°C (Hitachi F-4500, Tokyo, Japan)
242 using excitation and emission wavelengths of 563 and 586 nm, respectively, and slit
243 widths of 5 nm. For calibration, we added known amounts of H₂O₂ to the reaction
244 medium with mitochondrial samples.

245

246 **NAD(P) redox state**

247 We suspended the isolated liver mitochondria (0.5 mg · mL⁻¹) in a standard reaction
248 medium supplemented with 200 μ M EGTA, and 5 mM succinate plus 1 μ M rotenone,
249 and monitored the changes in the redox state of NAD(P) in a spectrofluorometer
250 (Hitachi F-7100) at 28°C, using excitation and emission wavelengths of 366 and 450
251 nm, respectively, and slit widths of 5 nm. Of note, only the reduced forms of NAD(P)
252 exhibit a strong endogenous fluorescence signal. The peroxide-metabolizing system
253 supported by NADPH was challenged with exogenous tert-butyl hydroperoxide (t-
254 BOOH), an organic peroxide that is metabolized through the glutathione
255 peroxidase/reductase system (Liu and Kehrer, 1996). As a reference, we added known
256 amounts of NADH to the reaction medium in the absence of mitochondria.

257

258 **Statistical analyses**

259 We tested for data normality and homoscedasticity by the Shapiro-Wilk and Barlett's
260 K-squared tests, respectively, using the R package. For variables that met the
261 assumptions of parametric tests, we performed a two-tailed unpaired *t*-test for
262 independent samples for comparison between fasted and fed. Whenever data failed the

263 premises, we compared the groups by the Mann-Whitney test. We performed all
264 analysis in Prism GraphPad software v. 7.1. We presented the results as mean and
265 standard error (s.e.m.), assuming the significance level of 0.05.

266

267 **RESULTS**

268

269 **Oxygen consumption of liver permeabilized tissue and isolated mitochondria**

270 Liver permeabilized tissue from fed snakes exhibited 30% higher V_{\max} than fasting
271 snakes (**Fig. 1A**, unpaired t -test, $P=0.0086$). Citrate synthase activity of liver
272 permeabilized tissue did not differ between the groups (**Fig. 1B**, unpaired t -test, $P<0.5$).
273 For isolated mitochondria, fed snakes exhibited 40%, 58% and 64% higher respiration
274 rates supported by complex I-linked substrates at basal, OXPHOS and, state 4_o,
275 respectively, in comparison to fasting snakes (**Fig. 2A, B**, t -test, $P\leq 0.05$). Mitochondrial
276 V_{\max} stimulated with complex I-linked substrates was 53% higher in the fed group (t -
277 test, $P\leq 0.05$), while mitochondrial V_{\max} stimulated with complex II- linked substrates
278 were not different between fasting and fed (**Fig. 2C**, t -test, $P=0.19$). Because *B.*
279 *constrictor* mitochondria were insensitive to both antimycin A and myxothiazol, we
280 could not block complex III activity and could not evaluate complex III and IV.
281 Mitochondrial respiratory control ratios and citrate synthase activity did not differ
282 between groups (**Fig. 2D, E**, Mann-Whitney, $P=0.45$).

283

284 **Assessment of mitochondrial Ca^{2+} retention capacity**

285 Ca^{2+} retention capacity was evaluated by sequential additions of Ca^{2+} pulses (**Fig. 3A,**
286 **B**) to the medium. Mitochondria of fasting and fed snakes exhibited similar capacities to
287 retain calcium. Mitochondria of fasting snakes were able to take and retain
288 approximately 264 ± 67 nmol $Ca^{2+} \cdot mg$ protein⁻¹ versus 465 ± 79 nmol $Ca^{2+} \cdot mg$
289 protein⁻¹ of fed snakes, (**Fig. 3C**, t -test, $P>0.05$). With the presence of CsA, both groups
290 of snakes similarly increased resistance to PTP opening (1140 ± 35 nmol $Ca^{2+} \cdot mg$
291 protein⁻¹ in the fasting group vs. 900 ± 173 nmol $Ca^{2+} \cdot mg$ protein⁻¹ in the fed group)
292 (**Fig. 3C**, Mann-Whitney, $P=0.30$).

293

294 **Mitochondrial hydrogen peroxide (H_2O_2) release and redox state of NAD(P)**

295 H_2O_2 released from liver mitochondria of fed snakes (76.5 ± 16.5 $\mu mol \cdot mg^{-1} \cdot min^{-1}$)
296 was 2-fold higher than from fasting snakes (36.8 ± 2.5 $\mu mol \cdot mg^{-1} \cdot min^{-1}$) (Mann-

297 Whitney, $P=0.02$) (**Fig. 4A, B**). There was no difference in the NADPH-dependent
298 capacity to metabolize peroxide in fasting versus fed snakes (**Fig. 4C, D**, t -test, $P=0.16$).

299

300 DISCUSSION

301

302 The present study revealed that *B. constrictor* liver mitochondria exhibit
303 profound energetic changes in response to meal intake. After feeding, mitochondrial
304 respiration rates from *B. constrictor* were significantly increased in comparison to unfed
305 snakes. Mitochondria are dynamic structures, ongoing fusion, fission processes, and
306 changes in number, morphology, and distribution, depending on the developmental,
307 physiological, and environmental conditions (Mishra and Chan, 2016).
308 Notwithstanding, the capacity to shift liver mitochondrial profiles two days after meal
309 intake in boas is remarkable, bringing attention to the underlying mechanisms and the
310 potential effects on mitochondria from other tissues directly or not involved in the
311 digestion and absorption processes *per se*.

312 We observed a remarkable increase of liver respiration rate during OXPHOS
313 (oxidative phosphorylation or state 3) of fed snakes compared to fasting, in the
314 magnitude of approximately 60%. This increase reflects what is reported for whole-
315 animal oxygen consumption rates (VO_2) in snakes but should consider the differences in
316 the meal size, the time spent at fasting, and the moment of post-feeding sampling. For
317 example, varying periods of fasting in *B. constrictor* did not change the total energetic
318 cost of digestion. However, it changed the temporal profile of the postprandial response
319 (de Figueiredo et al., 2020). The increase in respiration rates seems to be fueled by
320 substrates linked to complex I because we did not see differences in V_{max} between
321 fasting and fed snakes when using complex II-linked substrates. Indeed, upregulation of
322 genes for respiratory complex I, among other genes related to oxidative
323 phosphorylation, was reported during digestion in snakes (Duan et al., 2017).
324 Unfortunately, mitochondrial function studies in snakes are scarce. Interestingly, it was
325 found that low temperature can impact coupling and efficiency in liver mitochondria of
326 the snake *Natrix natrix*, but only when respiration was driven by succinate as the
327 respiratory substrate (Dubinin et al., 2019), indicating that different sources of stimulus
328 can impact mitochondrial function distinctly.

329 Another interesting finding was that feeding did not influence the quantity or
330 efficiency of *B. constrictor* liver mitochondria since citrate synthase activity and

331 respiratory control ratios were maintained. The mitochondria of fasting boas exhibited
332 lower respiratory rates in all measured states, following the low resting energetic
333 demand of the species (de Figueiredo et al., 2020; Stuginski et al., 2018). However, the
334 capacity to also exhibit a lower respiration rate after ATP synthase blockade with
335 oligomycin (state 4_o) indicates the capacity to reduce leakage of protons through the
336 membrane, which is a crucial contributing factor towards energy saving (Brand et al.,
337 1993), and probably to the low metabolic rates observed in ambush-hunting snakes
338 (Stuginski et al., 2018). Unfortunately, we could not determine the respiration induced
339 by the proton leak due to the lack of response to complex III inhibition. The
340 insensitivity to complex III inhibitors indicates that the ubiquinol-cytochrome c
341 oxidoreductase complex may exhibit a different molecular structure in snakes, as this
342 outcome was also observed in *Bothrops alternatus* (Ogo et al., 1993) and *Python regius*
343 (Bundgaard et al., 2020). Like boas, long-term fasting in king penguin chicks also did
344 not reduce skeletal muscle mitochondria efficiency compared to short-term fasting in
345 birds (Bourguignon et al., 2017). In contrast, fasting mammals exhibited the same or
346 even more significant proton leak than after feeding, compromising the efficiency of
347 mitochondria during food deprivation periods (Brown and Staples, 2011; Menezes-
348 Filho et al., 2019; Sorensen et al., 2006). Therefore, the capacity of lowering the
349 leakiness might imply an adaptation of the *B. constrictor* mitochondria to recurrent
350 fasting periods.

351 In contrast to findings from isolated mitochondria, maximal respiration rate
352 (V_{\max}) of permeabilized liver tissue was the only difference between our fasting and fed
353 boas. The different results obtained from liver isolated mitochondria and permeabilized
354 tissue could reflect intracellular interactions (Picard et al., 2010) or relate to different
355 bioenergetics profiles exhibited by mitochondrial subpopulations. Recently, a paper
356 investigating brown adipose tissue (BAT) mitochondria showed that when associated
357 with lipid droplets, mitochondria exhibited increased coupling, related to fatty acid
358 synthesis, in contrast to cytoplasmic mitochondria, which were related to fatty acid
359 oxidation (Benador et al., 2018). Interestingly, the bioenergetics results of the lipid
360 droplet subpopulation of mitochondria from BAT of Benador's work were similar to the
361 results obtained from *B. constrictor* of the fed treatment. Also, snakes preferentially
362 oxidize protein over lipids during the 14 days after feeding (McCue et al., 2015),
363 increasing the proportion of lipid droplet mitochondria compared to cytoplasmic
364 mitochondria in the liver during the postprandial period. Nevertheless, more work is

365 needed to investigate if there are bioenergetics differences from mitochondrial
366 subpopulations in boas.

367 The mitochondrial Ca^{2+} retention capacity is a proxy for evaluating susceptibility
368 of the mitochondrial permeability transition pore (PTP), a phenomenon characterized by
369 the Ca^{2+} -dependent opening of a non-specific pore in the inner mitochondrial
370 membrane. The PTP affects the structure and function of mitochondria, which is
371 ultimately related to cell death by apoptosis or necrosis and to many pathological
372 conditions (Vercesi et al., 2018). The amount of Ca^{2+} that leads to overload, thus
373 triggering PTP, varies with the source and conditions of mitochondria and the presence
374 of protectors or inducers acting on the still debated pore constitutional units
375 (Kowaltowski et al., 2001). Differently from mice mitochondria, which showed a higher
376 susceptibility to PTP when at fasting (Menezes-Filho et al., 2019), nutritional status
377 does not seem to affect the susceptibility to PTP in *B. constrictor*, as fasting and fed
378 snakes exhibited no differences in mitochondrial Ca^{2+} retention. PTP can be sensitized
379 by oxidative stress and oxidized NADPH (NADP^+) (Castilho et al., 1995; Vercesi et al.,
380 1988; Zago et al., 2000), as excess ROS increase oxidation of protein thiols and
381 promotes disulfide bonds and cross-linked protein aggregation in the inner
382 mitochondrial membrane (Castilho et al., 1995; Fagian et al., 1990; Valle et al., 1993;
383 Vercesi, 1984). However, as we will discuss further, we also did not observe changes in
384 NAD(P) redox status, and the increased rate of H_2O_2 production seems not to be leading
385 to oxidative stress, thus not influencing PTP sensibility.

386 Liver mitochondria from *B. constrictor* exhibited higher rates of H_2O_2 released
387 after ingestion of a meal compared to fasting, which contrasts with mitochondria from
388 fed mammals and a study in fasted fish. Rodent mitochondria and the brown trout
389 (*Salmo trutta*) exhibited higher levels of released H_2O_2 when subjected to fasting
390 (Menezes-Filho et al., 2019; Salin et al., 2018; Sorensen et al., 2006). The reduced H_2O_2
391 of fasting boas may be due to the low energetic demand during fasting in snakes
392 (Ensminger et al., 2021) and may be related to the remarkable capacity of metabolic
393 regulation in such animals (McCue, 2007). Nevertheless, a two-month period fasting in
394 *B. constrictor* may not be sufficient time to induce detrimental effects in mitochondria.
395 Ambush-hunting snakes were shown to possess lower metabolic rates than active
396 foraging snakes that feed more frequently (Stuginski et al., 2018), meaning that the
397 energetic costs could be sustained for long periods using stored energy reserves. For
398 example, the rattlesnake *Crotalus durissus* was shown to endure under 12 months of

399 food deprivation with slow body mass loss and no changes in resting VO₂ (Leite et al.,
400 2014). The increase in H₂O₂ could simply reflect the increase in aerobic metabolism and
401 seems to not directly lead to oxidative stress and damage because we observed no
402 differences in the redox status of NAD(P). Also, there is evidence that increased ROS
403 generation after feeding in snakes may be concurrent to increased antioxidant defense,
404 as genes encoding antioxidant enzymes like catalase, peroxiredoxin, glutathione
405 transferase, and heat shock protein were shown to be upregulated in digesting pythons
406 (Duan et al., 2017).

407 Studies are increasingly showing that ROS generation is not essentially
408 connected to damage, with demonstrations that ROS can act as signaling molecules,
409 playing an essential role in the crosstalk from mitochondria and nucleus to maintain cell
410 homeostasis (Shadel and Horvath, 2015). Of note, in mammals, there are remarkable
411 differences between an acute fasting event and chronic fasting regimes as intermittent
412 fasting (IF) or caloric restriction (CR) interventions. In both IF and CR, there is growing
413 evidence that chronic recurrent fasting regimes improve defenses against oxidative
414 stress and repair of damaged molecules (de Cabo and Mattson, 2019). In liver
415 mitochondria from rodents, caloric restriction did not affect respiration rates but reduced
416 ROS generation when energized with complex I-linked substrates and protected against
417 PTP (Lambert et al., 2004; López-Torres et al., 2002; Menezes-Filho et al., 2017). In *B.*
418 *constrictor*, which is adapted to recurrent fasting regimes, similar adaptive mechanisms
419 can be potentially operative. Nevertheless, more studies could be performed to carefully
420 evaluate the contrasting effects of transient beneficial effects of ROS and harmful
421 sustained elevated ROS levels in response to a fasting-feeding transition in snakes of
422 different feeding strategies.

423

424 **CONCLUDING REMARKS**

425 In summary, our results showed that liver mitochondria of *B. constrictor* possess
426 postprandial effects, exhibiting a rapid shift of mitochondrial bioenergetics towards
427 higher respiration rates and oxidative phosphorylation supported by complex I-linked
428 substrates, demonstrating the plasticity of snakes' mitochondrial function. Furthermore,
429 our results showed that mitochondrial function adaptations of boas might play a vital
430 role in the fasting and feeding transition and be pivotal in organismal fitness by
431 affecting animal performance.

432

433 **Acknowledgements**

434 The authors are thankful to Prof. Anibal E. Vercesi (University of Campinas, SP,
435 Brazil) for providing all the necessary facilities to conduct this research work, and to
436 “Centro de Recuperação de Animais Silvestres do Parque Ecológico do Tietê (CRAS,
437 São Paulo, SP, Brazil)”, for the provision of animals.

438

439 **Competing interests**

440 The authors declare no competing or financial interests.

441

442 **Author contributions**

443 Conceptualization: ALC, HRMA, MRS; Methodology: HRMA, MRS, CDCN; Formal
444 analysis: HRMA, MRS; Investigation: HRMA, MRS, CDCN; Resources: MRS, CDCN,
445 JEC; Writing - original draft: HRMA, MRS; Writing - review & editing: HRMA, MRS,
446 ALC, JEC; Supervision: ALC, JEC; Project administration: ALC, JEC; Funding
447 acquisition: ALC.

448

449 **Funding**

450 This study was supported by the Fundação de Amparo à Pesquisa do Estado da Bahia
451 (FAPESB), to HRMA and Instituto Nacional de Ciência e Tecnologia (INCT) em
452 Fisiologia Comparada (FAPESP, grant 08/57712-4). The following researches were
453 awarded by Fundação de Amparo à Pesquisa do Estado de São Paulo (FAPESP)
454 fellowships n. 2017/05487-6 to MRS and n. 2019/220855-7 to CDCN; and grants n.
455 2017/17728-8 to AEV and 2020/12962-5 to JEC.

456

457 **Reference list**

458

459 **Andrade, D. V., De Toledo, L. F., Abe, A. S. and Wang, T.** (2004). Ventilatory
460 compensation of the alkaline tide during digestion in the snake *Boa constrictor*. *J.*
461 *Exp. Biol.* **207**, 1379–1385.

462 **Benador, I. Y., Veliova, M., Mahdavian, K., Petcherski, A., Wikstrom, J. D.,**
463 **Assali, E. A., Acín-Pérez, R., Shum, M., Oliveira, M. F., Cinti, S., et al.** (2018).
464 Mitochondria bound to lipid droplets have unique bioenergetics, composition, and
465 dynamics that support lipid droplet expansion. *Cell Metab.* **27**, 869-885.e6.

466 **Benard, G., Faustin, B., Passerieux, E., Galinier, A., Rocher, C., Bellance, N.,**

- 467 **Delage, J. P., Casteilla, L., Letellier, T. and Rossignol, R.** (2006). Physiological
468 diversity of mitochondrial oxidative phosphorylation. *Am. J. Physiol. - Cell*
469 *Physiol.* **291**, 1172–1182.
- 470 **Bourguignon, A., Rameau, A., Toullec, G., Romestaing, C. and Roussel, D.** (2017).
471 Increased mitochondrial energy efficiency in skeletal muscle after long-term
472 fasting: Its relevance to animal performance. *J. Exp. Biol.* **220**, 2445–2451.
- 473 **Brand, M. D., Harper, M. E. and Taylor, H. C.** (1993). Control of the effective P/O
474 ratio of oxidative phosphorylation in liver mitochondria and hepatocytes. *Biochem.*
475 *J.* **291**, 739–748.
- 476 **Brown, J. C. L. and Staples, J. F.** (2011). Mitochondrial metabolic suppression in
477 fasting and daily torpor: Consequences for reactive oxygen species production.
478 *Physiol. Biochem. Zool.* **84**, 467–480.
- 479 **Brown, G. C., Lakin-Thomas, P. L. and Brand, M. D.** (1990). Control of respiration
480 and oxidative phosphorylation in isolated rat liver cells. *Eur. J. Biochem.* **192**,
481 355–362.
- 482 **Bundgaard, A., James, A. M., Harbour, M. E., Murphy, M. P. and Fago, A.** (2020).
483 Stable mitochondrial CICIII(2) supercomplex interactions in reptiles versus
484 homeothermic vertebrates. *J. Exp. Biol.* **223**, jeb223776.
- 485 **Busanello, E. N. B., Marques, A. C., Lander, N., de Oliveira, D. N., Catharino, R.**
486 **R., Oliveira, H. C. F. and Vercesi, A. E.** (2017). Pravastatin chronic treatment
487 sensitizes hypercholesterolemic mice muscle to mitochondrial permeability
488 transition: Protection by creatine or coenzyme Q10. *Front. Pharmacol.* **8**, 1–11.
- 489 **Butler, M. W., Lutz, T. J., Fokidis, H. B. and Stahlschmidt, Z. R.** (2016). Eating
490 increases oxidative damage in a reptile. *J. Exp. Biol.* **219**, 1969–1973.
- 491 **Castilho, R. F., Kowaltowski, A. J., Meinicke, A., Bechara, E. J. H. and Vercesi, A.**
492 **E.** (1995). Permeabilization of the inner mitochondrial membrane by Ca²⁺ ions is
493 stimulated by t-butyl hydroperoxide and mediated by reactive oxygen species
494 generated by mitochondria. *Free Radic. Biol. Med.* **18**, 479–486.
- 495 **Cruz-Neto, A. P., Andrade, D. V and Abe, A. S.** (1999). Energetic cost of predation:
496 Aerobic metabolism during prey ingestion by juvenile rattlesnakes, *Crotalus*
497 *durissus*. *J. Herpetol.* **33**, 229–234.
- 498 **de Cabo, R. and Mattson, M. P.** (2019). Effects of intermittent fasting on health,
499 aging, and disease. *N. Engl. J. Med.* **381**, 2541–2551.
- 500 **de Figueiredo, A. C., de Barros, F. C. and de Carvalho, J. E.** (2020). Effects of

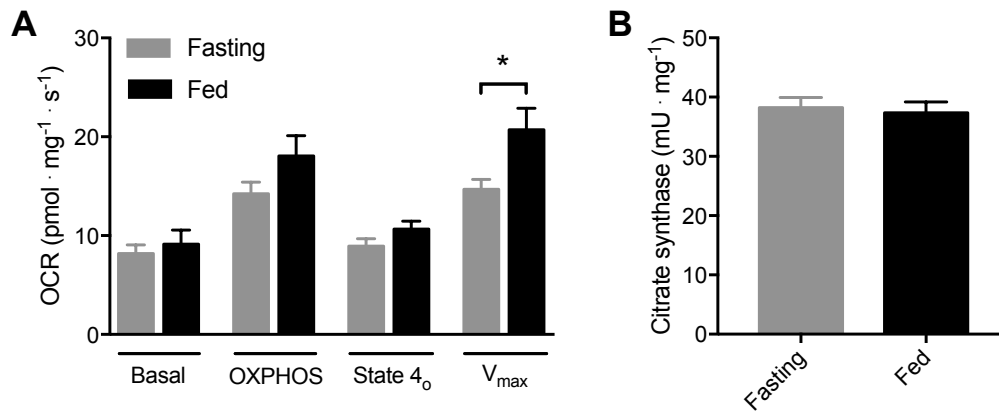
- 501 prolonged fasting on postprandial metabolic rates of *Boa constrictor* linnaeus 1758
502 (Serpentes: Boidae). *Herpetol. Notes* **13**, 621–625.
- 503 **Dejean, L., Beauvoit, B., Bunoust, O., Fleury, C., Guérin, B. and Rigoulet, M.**
504 (2001). The calorimetric-respirometric ratio is an on-line marker of enthalpy
505 efficiency of yeast cells growing on a non-fermentable carbon source. *Biochim.*
506 *Biophys. Acta - Bioenerg.* **1503**, 329–340.
- 507 **Duan, J., Sanggaard, K. W., Schauser, L., Lauridsen, S. E., Enghild, J. J.,**
508 **Schierup, M. H. and Wang, T.** (2017). Transcriptome analysis of the response of
509 Burmese python to digestion. *Gigascience* **6**, 1–18.
- 510 **Dubinín, M. V., Svinin, A. O., Vedernikov, A. A., Starinets, V. S., Tenkov, K. S.,**
511 **Belosludtsev, K. N. and Samartsev, V. N.** (2019). Effect of hypothermia on the
512 functional activity of liver mitochondria of grass snake (*Natrix natrix*): inhibition
513 of succinate-fueled respiration and K⁺ transport, ROS-induced activation of
514 mitochondrial permeability transition. *J. Bioenerg. Biomembr.* **51**, 219–229.
- 515 **Duchen, M. R.** (2000). Mitochondria and calcium: From cell signalling to cell death. *J.*
516 *Physiol.* **529**, 57–68.
- 517 **Dumas, J. F., Roussel, D., Simard, G., Douay, O., Foussard, F., Malthiery, Y. and**
518 **Ritz, P.** (2004). Food restriction affects energy metabolism in rat liver
519 mitochondria. *Biochim. Biophys. Acta - Gen. Subj.* **1670**, 126–131.
- 520 **Ensminger, D. C., Salvador-Pascual, A., Arango, B. G., Allen, K. N. and Vázquez-**
521 **Medina, J. P.** (2021). Fasting ameliorates oxidative stress: A review of
522 physiological strategies across life history events in wild vertebrates. *Comp.*
523 *Biochem. Physiol. -Part A Mol. Integr. Physiol.* **256**,
- 524 **Fagian, M. M., Pereira-da-Silva, L., Martins, I. S. and Vercesi, A. E.** (1990).
525 Membrane protein thiol cross-linking associated with the permeabilization of the
526 inner mitochondrial membrane by Ca²⁺ plus prooxidants. *J. Biol. Chem.* **265**,
527 19955–19960.
- 528 **Gavira, R. S. B. and Andrade, D. V.** (2013). Meal size effects on the postprandial
529 metabolic response of *Bothrops alternatus* (Serpentes: Viperidae). *Zoologia* **30**,
530 291–295.
- 531 **Hamanaka, R. B. and Chandel, N. S.** (2010). Mitochondrial reactive oxygen species
532 regulate cellular signaling and dictate biological outcomes. *Trends Biochem. Sci.*
533 **35**, 505–513.
- 534 **Kleiber, M.** (1961). *The Fire of Life: An introduction to animal energetics*. 453 p.

- 535 Wiley and Sons.
- 536 **Kowaltowski, A. J., Castilho, R. F. and Vercesi, A. E.** (2001). Mitochondrial
537 permeability transition and oxidative stress. *FEBS Lett.* **495**, 12–15.
- 538 **Kuznetsov, A. V., Veksler, V., Gellerich, F. N., Saks, V., Margreiter, R. and Kunz,**
539 **W. S.** (2008). Analysis of mitochondrial function in situ in permeabilized muscle
540 fibers, tissues and cells. *Nat. Protoc.* **3**, 965–976.
- 541 **Lambert, A. J., Wang, B., Yardley, J., Edwards, J. and Merry, B. J.** (2004). The
542 effect of aging and caloric restriction on mitochondrial protein density and oxygen
543 consumption. *Exp. Gerontol.* **39**, 289–295.
- 544 **Leite, C. A. C., Wang, T., Taylor, E. W., Abe, A. S., Leite, G. S. P. C. and de**
545 **Andrade, D. O. V.** (2014). Loss of the ability to control right-to-left shunt does
546 not influence the metabolic responses to temperature change or long- term fasting
547 in the South American rattlesnake *Crotalus durissus*. *Physiol. Biochem. Zool.* **87**,
548 568–575.
- 549 **Liu, H. and Kehrer, J. P.** (1996). The reduction of glutathione disulfide produced by t-
550 butyl hydroperoxide in respiring mitochondria. *Free Radic. Biol. Med.* **20**, 433–
551 442.
- 552 **López-Torres, M., Gredilla, R., Sanz, A. and Barja, G.** (2002). Influence of aging
553 and long-term caloric restriction on oxygen radical generation and oxidative DNA
554 damage in rat liver mitochondria. *Free Radic. Biol. Med.* **32**, 882–889.
- 555 **McCue, M. D.** (2007). Snakes survive starvation by employing supply- and demand-
556 side economic strategies. *Zoology* **110**, 318–327.
- 557 **McCue, M. D.** (2008). Extreme starvation tolerance in snakes: a model system for
558 resource limitation.
- 559 **McCue, M. D. and Pollock, E. D.** (2008). Stable isotopes may provide evidence for
560 starvation in reptiles. *Rapid Commun. Mass Spectrom.* **22**, 2307–2314.
- 561 **McCue, M. D., Lillywhite, H. B. and Beaupre, S. J.** (2012). Physiological Responses
562 to Starvation in Snakes: Low Energy Specialists BT - Comparative Physiology of
563 Fasting, Starvation, and Food Limitation. In (ed. McCue, M. D.), pp. 103–131.
564 Berlin, Heidelberg: Springer Berlin Heidelberg.
- 565 **McCue, M. D., Guzman, R. M. and Passemont, C. A.** (2015). Digesting pythons
566 quickly oxidize the proteins in their meals and save the lipids for later. *J. Exp. Biol.*
567 **218**, 2089–2096.
- 568 **Menezes-Filho, S. L., Amigo, I., Prado, F. M., Ferreira, N. C., Koike, M. K., Pinto,**

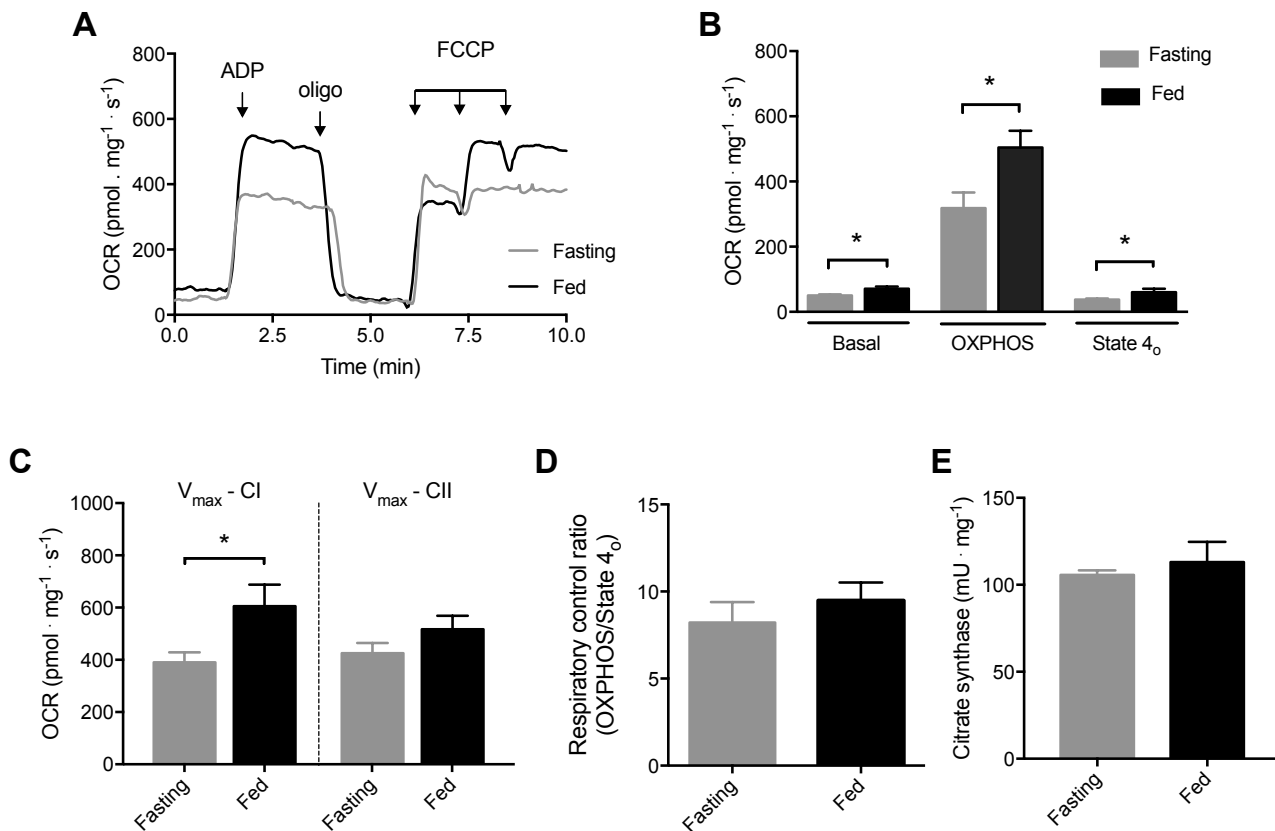
- 569 **I. F. D., Miyamoto, S., Montero, E. F. S., Medeiros, M. H. G. and**
570 **Kowaltowski, A. J.** (2017). Caloric restriction protects livers from
571 ischemia/reperfusion damage by preventing Ca²⁺-induced mitochondrial
572 permeability transition. *Free Radic. Biol. Med.* **110**, 219–227.
- 573 **Menezes-Filho, S. L., Amigo, I., Luévano-Martínez, L. A. and Kowaltowski, A. J.**
574 (2019). Fasting promotes functional changes in liver mitochondria. *Biochim.*
575 *Biophys. Acta - Bioenerg.* **1860**, 129–135.
- 576 **Mishra, P. and Chan, D. C.** (2016). Metabolic regulation of mitochondrial dynamics.
577 *J. Cell Biol.* **212**, 379–387.
- 578 **Miwa, S., Treumann, A., Bell, A., Vistoli, G., Nelson, G., Hay, S. and Von**
579 **Zglinicki, T.** (2016). Carboxylesterase converts Amplex red to resorufin:
580 Implications for mitochondrial H₂O₂ release assays. *Free Radic. Biol. Med.* **90**,
581 173–183.
- 582 **Ogo, S. H., Bernardes, C. F., Glass, M. I., Torsoni, M. . and Vercesi, A. E.** (1993).
583 Functional mitochondria in snake *Bothrops alternatus* erythrocytes and modulation
584 of HbO₂ affinity by mitochondrial ATP. *J Comp Physiol B* **163**, 614–619.
- 585 **Picard, M., Ritchie, D., Wright, K. J., Romestaing, C., Thomas, M. M., Rowan, S.**
586 **L., Taivassalo, T. and Hepple, R. T.** (2010). Mitochondrial functional
587 impairment with aging is exaggerated in isolated mitochondria compared to
588 permeabilized myofibers. *Aging Cell* **9**, 1032–1046.
- 589 **Rolfe, D. F. and Brown, G. C.** (1997). Cellular energy utilization and molecular origin
590 of standard metabolic rate in mammals. *Physiol. Rev.* **77**, 731–758.
- 591 **Ronchi, J. A., Figueira, T. R., Ravagnani, F. G., Oliveira, H. C. F., Vercesi, A. E.**
592 **and Castilho, R. F.** (2013). A spontaneous mutation in the nicotinamide
593 nucleotide transhydrogenase gene of C57BL/6J mice results in mitochondrial
594 redox abnormalities. *Free Radic. Biol. Med.* **63**, 446–456.
- 595 **Roussel, D., Boël, M., Mortz, M., Romestaing, C., Duchamp, C. and Voituron, Y.**
596 (2019). Threshold effect in the H₂O₂ production of skeletal muscle mitochondria
597 during fasting and refeeding. *J. Exp. Biol.* **222**,.
- 598 **Salin, K., Villasevil, E. M., Anderson, G. J., Auer, S. K., Selman, C., Hartley, R. C.,**
599 **Mullen, W., Chinopoulos, C. and Metcalfe, N. B.** (2018). Decreased
600 mitochondrial metabolic requirements in fasting animals carry an oxidative cost.
601 *Funct. Ecol.* **32**, 2149–2157.
- 602 **Sartori, M. R., Lerchner, J., Castilho, R. F., Volpe, P. O., Mertens, F. and Vercesi,**

- 603 **A. E.** (2021). Chip-calorimetric assessment of heat generation during Ca^{2+} uptake
604 by digitonin-permeabilized *Trypanosoma cruzi*. *J. Therm. Anal. Calorim.*
- 605 **Schieber, M. and Chandel, N. S.** (2014). ROS function in redox signaling and
606 oxidative stress. *Curr. Biol.* **24**, R453–R462.
- 607 **Secor, S. M.** (2009). Specific dynamic action: A review of the postprandial metabolic
608 response. *J. Comp. Physiol. B Biochem. Syst. Environ. Physiol.* **179**, 1–56.
- 609 **Secor, S. M. and Diamond, J.** (1997). Effects of meal size on postprandial responses in
610 juvenile Burmese pythons (*Python molurus*). *Am. J. Physiol. Integr. Comp.*
611 *Physiol.* **272**, R902–R912.
- 612 **Secor, S. M. and Diamond, J.** (1998). A vertebrate model of extreme physiological
613 regulation. *Nature* **395**, 659–662.
- 614 **Secor, S. M. and Diamond, J. M.** (2000). Evolution of regulatory responses to feeding
615 in snakes. *Physiol. Biochem. Zool.* **73**, 123–141.
- 616 **Shadel, G. S. and Horvath, T. L.** (2015). Mitochondrial ROS signaling in organismal
617 homeostasis. *Cell* **163**, 560–569.
- 618 **Shepherd, D. and Garland, P. B.** (1969). The kinetic properties of citrate synthase
619 from rat liver mitochondria. *Biochem. J.* **114**, 597–610.
- 620 **Sorensen, M., Sanz, A., Gómez, J., Pamplona, R., Portero-Otín, M., Gredilla, R.**
621 **and Barja, G.** (2006). Effects of fasting on oxidative stress in rat liver
622 mitochondria. *Free Radic. Res.* **40**, 339–347.
- 623 **Starck, J. M. and Beese, K.** (2001). Structural flexibility of the intestine of burmese
624 python in response to feeding. *J. Exp. Biol.* **204**, 325–335.
- 625 **Stuginski, D. R., Navas, C. A., de Barros, F. C., Camacho, A., Bicudo, J. E. P. W.,**
626 **Grego, K. F. and de Carvalho, J. E.** (2018). Phylogenetic analysis of standard
627 metabolic rate of snakes: a new proposal for the understanding of interspecific
628 variation in feeding behavior. *J. Comp. Physiol. B Biochem. Syst. Environ. Physiol.*
629 **188**, 315–323.
- 630 **Toledo, L. F., Abe, A. S. and Andrade, D. V.** (2003). Temperature and meal size
631 effects on the postprandial metabolism and energetics in a boid snake. *Physiol.*
632 *Biochem. Zool.* **76**, 240–246.
- 633 **Valle, V. G. R., Fagian, M. M., Parentoni, L. S., Meinicke, A. R. and Vercesi, A. E.**
634 (1993). The participation of reactive oxygen species and protein thiols in the
635 mechanism of mitochondrial inner membrane permeabilization by calcium plus
636 prooxidants. *Arch. Biochem. Biophys.* **307**, 1–7.

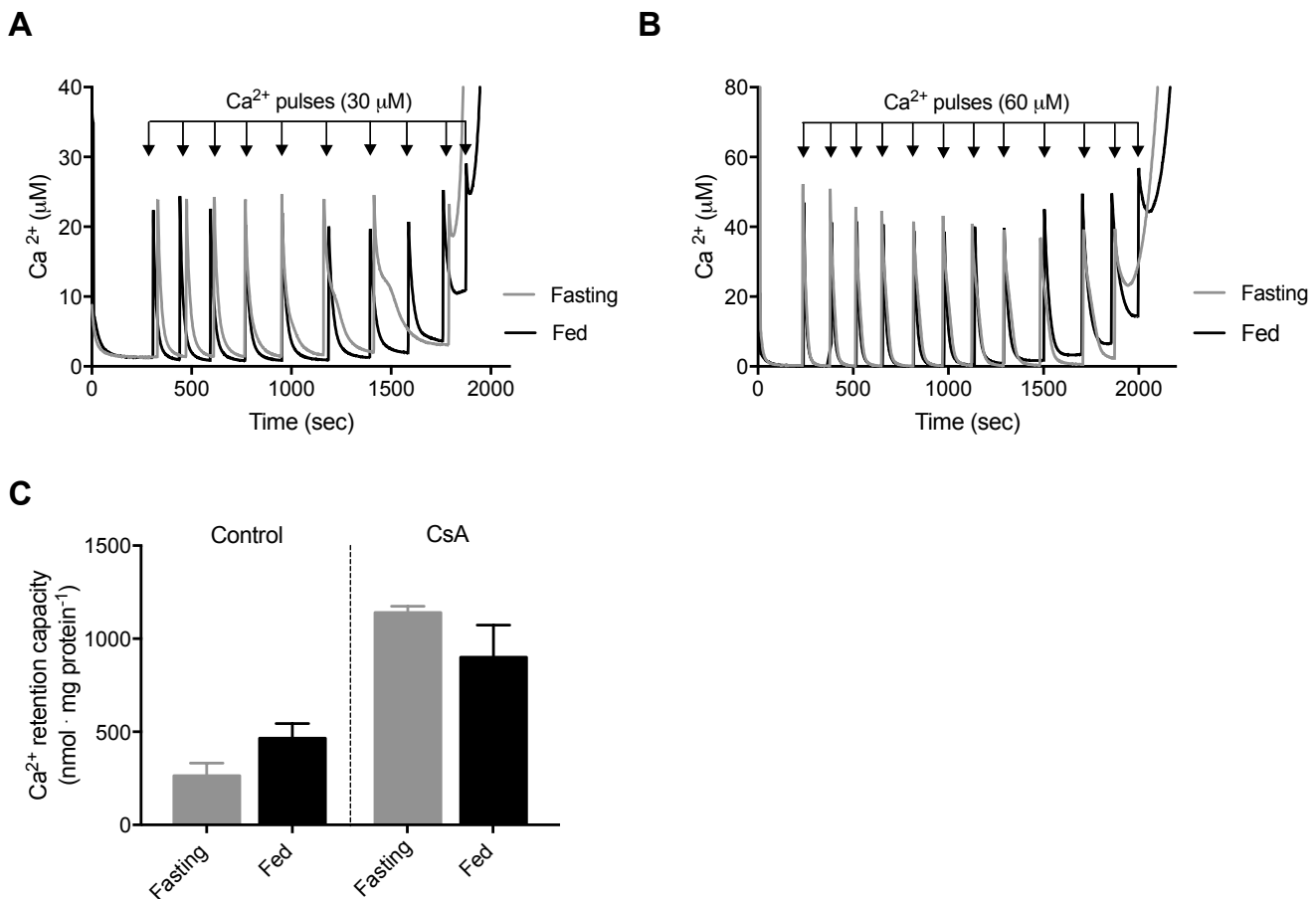
- 637 **Vercesi, A. E.** (1984). Possible participation of membrane thiol groups on the
638 mechanism of NAD(P)⁺-stimulated Ca²⁺ efflux from mitochondria. *Biochem.*
639 *Biophys. Res. Commun.* **119**, 305–310.
- 640 **Vercesi, A. E., Ferraz, V. L., Macedo, D. V and Fiskum, G.** (1988). Ca²⁺-dependent
641 NAD(P)⁺-induced alterations of rat liver and hepatoma mitochondrial membrane
642 permeability. *Biochem. Biophys. Res. Commun.* **154**, 934–941.
- 643 **Vercesi, A. E., Castilho, R. F., Kowaltowski, A. J., de Oliveira, H. C. F., de Souza-**
644 **Pinto, N. C., Figueira, T. R. and Busanello, E. N. B.** (2018). Mitochondrial
645 calcium transport and the redox nature of the calcium-induced membrane
646 permeability transition. *Free Radic. Biol. Med.* **129**, 1–24.
- 647 **Zago, E. B., Castilho, R. F. and Vercesi, A. E.** (2000). The redox state of endogenous
648 pyridine nucleotides can determine both the degree of mitochondrial oxidative
649 stress and the solute selectivity of the permeability transition pore. *FEBS Lett.* **478**,
650 29–33.
- 651



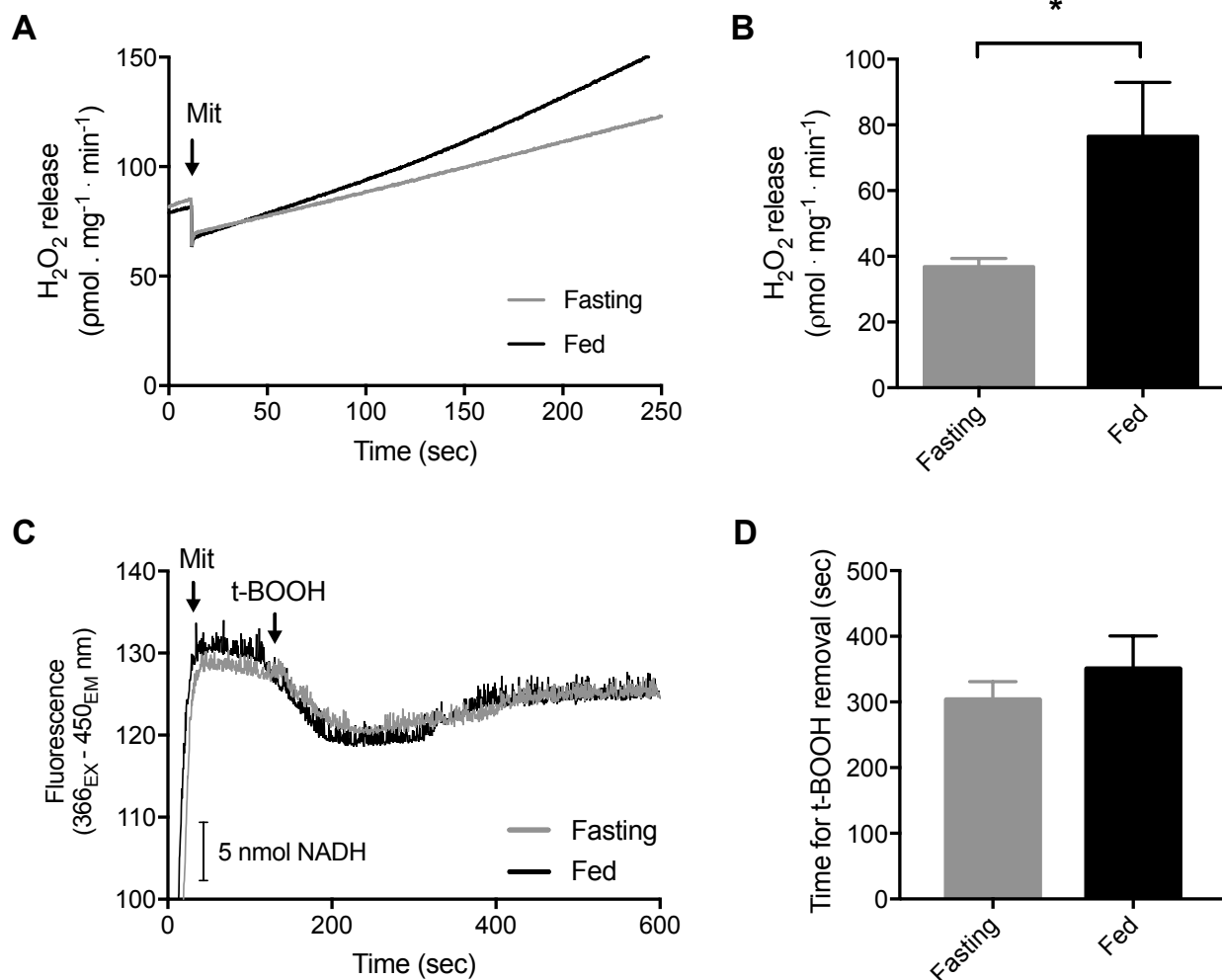
652 **Fig. 1 Feeding increased maximal respiration rate in liver permeabilized tissue**
653 **from *B. constrictor* snakes. A)** Oxygen consumption of liver permeabilized tissue at
654 the presence of 5 mM malate, 10 mM pyruvate, and 10 mM glutamate as substrates
655 (basal), after additions of 400 μ M ADP (OXPHOS), 1 μ g/ml oligomycin (State 4_o), and
656 0.8 μ M FCCP (V_{max}). **B)** Citrate synthase activity. Bars denotes means \pm s.e.m.; *
657 $P < 0.01$, t -test (N = 17 fasting, N = 11 fed; independent experiments).



658 **Fig. 2 Feeding increased *B. constrictor* basal respiration, oxidative phosphorylation**
 659 **capacity, state 4_o and V_{max} in liver isolated mitochondria energized with complex I-**
 660 **linked substrates. A)** Representative traces of oxygen consumption rate (OCR) of
 661 fasting and fed snakes, in the presence of 1 mM malate, 2.5 mM pyruvate and 2.5 mM
 662 glutamate as substrates, with additions of 300 μM ADP, 1 μg/ml oligomycin (oligo) and
 663 50 ηM FCCP, where indicated by the arrows. **B)** Quantification of OCR per mg
 664 mitochondrial protein; * $P \leq 0.5$, t -test; **C)** Maximal respiration rate (V_{max}) stimulated
 665 with complex-I and complex-II linked substrates; * $P \leq 0.5$, t -test; **D)** Respiratory control
 666 ratios (OXPHOS/State 4_o); **E)** Citrate synthase activity. Data are presented as means ±
 667 s.e.m. (N = 5 fasting, N = 4 fed).



668 **Fig. 3 Feeding did not affect mitochondrial Ca^{2+} retention capacity in *B. constrictor***
669 **snakes.** After addition of mitochondria to the system, Ca^{2+} retention capacity was
670 accessed by consecutive additions of Ca^{2+} pulses until Ca^{2+} -induced Ca^{2+} release as the
671 consequence of the opening of PTP. Representative traces are depicted in **A**) control
672 condition, Ca^{2+} pulses of 30 μM ; **B**) in the presence of cyclosporine A (CsA), Ca^{2+}
673 pulses of 60 μM . **C**) Amount of Ca^{2+} retained in each condition before the onset of
674 permeability transition. Data are presented as means \pm s.e.m., (N = 5 fasting, N = 4 fed).



675 **Fig 4. Liver mitochondria from fed individuals exhibited higher rates of H₂O₂**
676 **release but no evidence of oxidative stress in comparison to fasting individuals. A)**
677 **Representative traces of H₂O₂ release assayed by the Amplex™ UltraRed probe in**
678 **fasting (grey line) and fed (black line) liver mitochondria during resting respiratory state**
679 **supported by complex I substrates. B) H₂O₂ released at a basal state (*P=0.03, Mann-**
680 **Whitney test). C) Representative traces of the endogenous fluorescence of NAD(P) in**
681 **the reduced state monitored over time in mitochondria incubated in standard reaction**
682 **medium supplemented with succinate and rotenone in the absence of exogenous ADP;**
683 **D) Time spent to recover the reduced state of NAD(P) following the addition of 2.5 μM**
684 **organic peroxide (t-BOOH) load. The recovery time was used to indirectly estimate the**
685 **rate of peroxide removal in each group and the ability of mitochondria to scavenge**
686 **peroxide. Data are presented as means ± s.e.m. (N = 5 fasting, N = 4 fed).**